A slow atom source using a collimated effusive oven and a single-layer variable pitch coil Zeeman slower

S. C. Bell, M. Junker, M. Jasperse, L. D. Turner, Y.-J. Lin et al.

Citation: Rev. Sci. Instrum. **81**, 013105 (2010); doi: 10.1063/1.3276712
View online: http://dx.doi.org/10.1063/1.3276712
View Table of Contents: http://rsi.aip.org/resource/1/RSINAK/v81/i1
Published by the American Institute of Physics.

A slow atom source using a collimated effusive oven and a single-layer variable pitch coil Zeeman slower

S. C. Bell,[1] M. Junker,[1] M. Jasperse,[1] L. D. Turner,[2] Y.-J. Lin,[3] I. B. Spielman,[3] and R. E. Scholten[1,a)]

[1]*ARC Centre of Excellence for Coherent X-ray Science, School of Physics, The University of Melbourne, Victoria 3010, Australia*

[2]*School of Physics, Monash University, Victoria 3800, Australia*

[3]*Joint Quantum Institute, National Institute of Standards and Technology and University of Maryland, Gaithersburg, Maryland 20899, USA*

(Received 23 September 2009; accepted 30 November 2009; published online 22 January 2010)

We describe a simple slow atom source for loading a rubidium magneto-optical trap. The source includes an effusive oven with a long heated collimation tube. Almost all components are standard vacuum parts. The heating elements and thermocouples are external to the vacuum, protecting them from the hostile hot alkali environment and allowing repair without breaking vacuum. The thermal source is followed by a Zeeman slower with a single-layer coil of variable winding pitch. The single-layer design is simple to construct and has low inductance which allows for rapid switching of the magnetic field. The coil pitch was determined by fitting the analytic form of the magnetic field for a variable winding pitch to the desired magnetic field profile required to slow atoms. The measured magnetic field for the constructed coil is in excellent agreement with the desired field. The source produces atoms at 35 m/s with a flux up to 2×10^{10} cm^{-2} s^{-1} at 200 °C. © *2010 American Institute of Physics.* [doi:10.1063/1.3276712]

I. INTRODUCTION

Continuous slow-atom sources are important for loading magneto-optic traps (MOTs),[1,2] particularly when those traps form the first stage of experiments in degenerate quantum gases, where large initial numbers of cold atoms are needed due to losses in subsequent stages of evaporative cooling.[3] Most slow atom sources are either effusive ovens with Zeeman slowers, or variations on a MOT, which capture atoms from a thermal vapor, such as a low-velocity intense source[4] or a 2D+MOT.[5] The relative merits of each approach have been described elsewhere.[6,7]

We present a high-flux slow atom source designed for reliability, ease of fabrication, and longevity, based on a collimated effusive oven followed by a Zeeman slower. The oven was almost entirely constructed from standard vacuum components. External mounting of the heating elements and thermocouple sensors separates them from the harsh hot alkali environment and allows for easy replacement without breaking vacuum. Two implementations of the design (NIST and Melbourne) have achieved comparable performance, and one has been operational without breaking vacuum for 3 years.[8]

II. APPARATUS

Figure 1 is a schematic of the oven and zero-crossing Zeeman slower. Atoms effusing from the oven were collimated by a heated tube and a cold aperture. The atoms were then decelerated along the Zeeman slower and detected using either fluorescence or absorption from a probe laser beam.

A. Effusive oven

Effusive ovens are typically wasteful with most of the emitted atoms lost into a large solid angle, while only a small central portion of the beam is used. We have previously used rubidium candlestick recirculating ovens to extend the operating lifetime,[9–11] but they are relatively complicated to construct, difficult to load with rubidium, and unreliable in establishing proper wicking and recirculating action. Failure of in-vacuum heating elements and thermocouples also caused major loss of operating time. In the design presented here, we use a long collimation tube at elevated temperature which collects atoms emitted at large angles to the central beam axis, which are then re-emitted back to the reservoir or into the central flux.[12]

Figure 2 shows the oven section in greater detail. The alkali reservoir was formed from mini-conflat (DN16CF knife-edge flange) bellows,[13] containing a standard 5 g glass ampule of rubidium. After evacuating and baking the apparatus, the bellows were flexed to break the ampule. The bellows section was wrapped with a heating tape, typically run at a power of 12 W to raise the temperature to 80 °C, measured with a thermocouple attached directly to the bellows. The vapor pressure and mean free path were calculated to be 6×10^{-5} mbar and 0.75 m, respectively, indicating molecular flow conditions.

Atoms effused from the reservoir into a 10 mm diameter, 200 mm long stainless steel collimation tube, heated to 120 °C, well above the melting point of rubidium (39 °C).

a)Electronic mail: scholten@unimelb.edu.au.

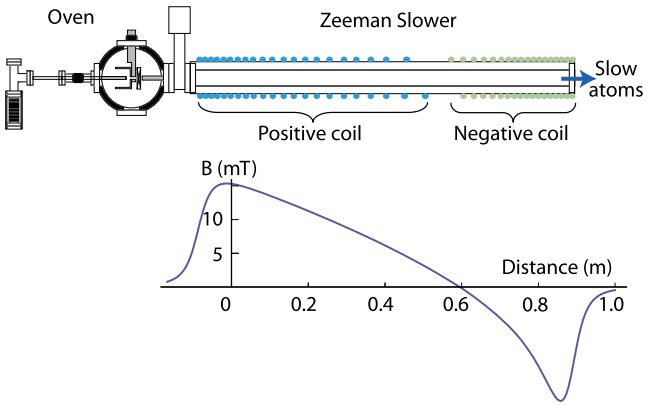

FIG. 1. (Color online) Schematic of the atomic source. Atoms effusing from the reservoir were collimated by a long hot tube and cold aperture, before entering the Zeeman slower. A positive and negative coil combine to form a zero-crossing Zeeman slower with magnetic field profile as shown.

An atom colliding with the hot wall of the tube can be re-emitted with some probability that the new trajectory will be within the exit solid angle of the collimation tube.[12] We calculate a 25× improvement in oven lifetime for the required flux into the capture region of the MOT, compared with a simple effusive aperture producing the same flux.

Atoms emerging off-axis from the collimation tube were captured by a cold cup. The cup was cooled by Peltier effect thermoelectric cooling devices external to the vacuum system, via a solid copper electrical feedthrough of 9.5 mm diameter, to −30 °C and more recently to −45 °C with a double-stage cooler. To reduce the residual background vapor load in the science chamber, a mechanical shutter blocked the exit of the cold cup except when atoms were needed for loading the MOT. A commercial shutter[14] and one made from the hard-drive of a digital audio player[15] have both been used successfully. A 70 mm length of 9.5 mm diameter pinch-off tube[16] separated the source from the Zeeman slower and main chamber for differential pumping with a calculated conductance of 1.3 l/s. A gate valve allowed for isolation of the oven for reloading if needed. The oven chamber was pumped with a 60 l/s diode ion pump, to a pressure of 10^{-9} mbar during operation. The ion pump was maintained at 70 °C, and the cold cup at −30 °C, to protect

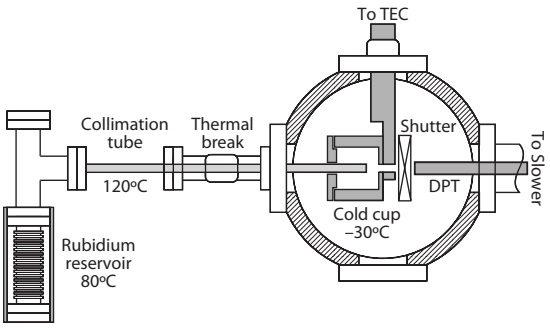

FIG. 2. Schematic diagram of the oven. Atoms effusing from the heated rubidium reservoir (80 °C) were collimated by the heated stainless steel collimation tube (120 °C) and cold cup aperture (−30 °C). The cold cup and mechanical shutter were used to minimize contamination of the vacuum pump and reduce the background gas load on the Zeeman slower, separated from the source by a differential pumping tube (DPT).

against alkali poisoning.[8] We observed a gradual increase in pressure by one order of magnitude over the 3 years of operation of the NIST source. Heating the ion pump to 150 °C for one week, while the cold cup was kept cold, restored the pressure.

B. Zeeman slower

The magnetic field required to keep atoms on resonance with the laser along the Zeeman slower is derived by assuming constant deceleration and equating the Doppler shift with the Zeeman shift:[17–19]

$$B_{\text{ideal}}(z) = B_a - \frac{\hbar k}{\mu'}\sqrt{v_0^2 - 2\eta a z}, \tag{1}$$

where v_0 is the peak velocity of atoms that are slowed, $a = \hbar k\Gamma/2m$ is the deceleration due to on-resonance photon scattering (assuming saturation of the transition), m is the mass of the atom, k is the wave number of the slowing laser, and Γ is the natural line width of the transition. The net gyromagnetic ratio $\mu' = \mu_B(g_e m_e - g_g m_g)$, where μ_B is the Bohr magneton, $g_{g,e}$ are the Landé g-factors and $m_{g,e}$ are the Zeeman quantum numbers for the ground or excited states. $\eta < 1$ is a design parameter that specifies the ratio of deceleration to the optimum deceleration, for example, to allow for limited laser power or imperfections in the magnetic field gradient that would otherwise decouple atoms from the slowing laser. B_a is a bias field which can be used to minimize transitions to optically dark states[20] or as in our case to design for a zero crossing in the magnetic field profile.[10,21]

The zero-crossing configuration offers several practical advantages. The magnetic field is divided into positive and negative regions (Fig. 1), such that the absolute field maxima are reduced, without changing the overall differential that defines the total atomic deceleration. The power dissipated is therefore also reduced by a factor of approximately 4. The atoms exit from a nonzero field, quickly decoupling from the slowing laser to preserve the narrow velocity distribution.[21–23] The arbitrary position of the zero crossing can be chosen to match the detuning of the slowing laser to a convenient frequency reference. Finally, the zero crossing allows for an additional vacuum pump between the two coils for increased pumping speed.[24]

Zero-crossing slowers also have potential drawbacks. First, in the negative field region, there are level-crossings at specific magnetic field strengths, where two states become degenerate.[20,25] In particular for ^{85}Rb, the $5P_{3/2}F=4$, $m_F=-4$ and $F=3$, $m_F=-2$ cross at 5.1 mT,[26] allowing loss from the cycling transition if the slowing laser polarization is imperfect. With a nonzero-crossing slower, these level crossings can be avoided, for example, by adding a bias such that the magnetic field is always greater than the level crossing fields.[19,25] Second, stray magnetic fields in the zero-crossing region may lead to precession of the atomic spin away from the slowing axis, on average reducing the dipole coupling to the light field. This may cause the deceleration to become insufficient for the atoms to remain coupled to the slowing light field. External magnetic fields at the zero crossing should therefore be carefully minimized with shielding or compensation coils, and/or the power of the slowing laser

beam should be high enough to ensure that atoms are continually optically pumped into the stretched state and thus polarized along the slowing axis. We found that the loss of atoms from the cycling transition was acceptable with a repump laser beam of modest power and careful adjustment of the polarization of slowing and repump light fields.

C. Coil with variable winding pitch

The magnetic field for a Zeeman slower is typically generated by a solenoid with a varying number of layers. The field of the stacked layer design can be calculated by assuming each turn is a single current-carrying loop and then summing the magnetic field contribution from each turn.[27] The field strength is discretized in layer steps. At each transition between layers, the field gradient is not optimal, leading to decoupling of some atoms from the slowing light field if η is high. The discretization effects are minimized by using a larger number of layers, reducing the required current. However, more layers increase the inductance and the coil becomes large, heavy, and time-consuming to construct. Alterations are difficult after assembly, as each turn is typically epoxied in place.

We used a single-layer helix with a varying winding pitch to create the necessary field profile. With only one layer, the coil was compact and light with low inductance, allowing for fast switching of the magnetic field. The single layer design could be wound very easily, and alterations or adjustments were possible after construction. A high current was needed to generate the necessary field, but the requirements ($\approx$100 A) were not extreme.

We modeled the helical coils with varying pitch using the following parametric equations:

$$\mathbf{r}(p) = [x(p), y(p), z(p)],$$

$$x(p) = R\cos\theta(p),$$

$$y(p) = R\sin\theta(p),$$

$$z(p) = c_7 p + c_8,$$

$$\theta(p) = \sum_{m=0\cdots6} c_m p^m, \tag{2}$$

where $p \in [0, 2\pi]$ is the free parameter; z is the distance along the coil; x, y are the transverse coordinates relative to the longitudinal coil axis; and R is the (fixed) radius of the coil. θ is the azimuthal angle of the coil, which we defined using a sixth-order polynomial in terms of the parameter p and seven coefficients $c_0 - c_6$. The distance along the coil z is linear in p with coefficients c_7, c_8. The field for a coil described by these equations was determined analytically at coordinates $\mathbf{r}' = \mathbf{r} + (0, 0, z')$ using the Biot–Savart law

$$\mathbf{B}_{\text{helix}}(z') = \frac{\mu I}{4\pi}\int_0^{2\pi} \frac{(d\mathbf{r}'/dp) \times \mathbf{r}'}{r'^3} dp, \tag{3}$$

for current I, where μ is the magnetic permeability, $d\mathbf{r}'$ is an incremental segment of wire along the helix, and $\mathbf{r}'$ is a vector from that segment to the location z' along the coil axis. The radial components cancel due to symmetry, so the integral can be simplified by only computing $B_{\text{helix},z}$, the z-component of the field on-axis. The cancellation of radial components is only strictly valid along the axis and to the extent that the helix is tightly wound. It is not valid at the ends, where the first and last turns do not have the full 2π circular symmetry.

TABLE I. Coefficients of Eq. (2) for the final coil design to produce the necessary field profile given by Eq. (1) for a current of I=110 A in each coil and a coil radius of R=38.3 mm. Values indicated by $\rightarrow$ were fixed to satisfy boundary conditions.

	Positive coil	Negative coil
c_0	$\rightarrow 0$	$\rightarrow \pi$
c_1	2.999 42	−1.999 5
c_2	8.698 12	−1.257 28
c_3	−0.302 31	−0.230 45
c_4	$\rightarrow 0$	0.020 38
c_5	0.001 58	0.003 47
c_6	$\rightarrow 0$	−0.001 20
c_7	−0.106 26	−0.043 08
c_8	0.581 49	0.618 19

It is important that the magnetic field falls to zero as quickly as possible outside the Zeeman slower to minimize the influence on the MOT fields, and to quickly decouple atoms from the slowing light field so that the narrow velocity distribution is preserved.[23] The magnetic field of the tapered coil was therefore fitted to a modified ideal profile (B_{aug}): the ideal slowing field (B_{ideal}) defined by Eq. (1) inside the slowing region and augmented with a $1/r^2$ decay outside the slowing region at either end. The $1/r^2$ decay fields were obtained by modeling a single coil running sufficient current to generate a field equal to the maximum at each end of the coil.

The fitting was also constrained by the physical dimensions of our system. The coil windings were spaced by more than the wire diameter of 4 mm and the total length of the coil was allowed to vary but was limited to 975 mm by the length of a pre-existing vacuum tube. The zero crossing was chosen at 0.59 m so that the slowing laser could be set with a detuning of −260 MHz relative to the zero velocity cooling transition. The detuning was chosen such that the slowing laser and repump were off-resonant with all hyperfine states of atoms trapped in the MOT and convenient for locking the slowing laser to a saturated absorption crossover 90 MHz below the cooling transition with a double-pass 85 MHz acousto-optic modulator.

The positive and negative sections of the slowing magnetic field were generated by two separate helical windings with the same helicity but opposing currents. The coefficients of the parametric equations for the helix, $c_0 - c_8$, were determined from a nonlinear fit of the z-component of the on-axis magnetic field solution of Eq. (3), $B_{\text{helix},z}$ to the augmented ideal magnetic field profile for a Zeeman slower, B_{aug}. The coefficients obtained are shown in Table I.

Figure 3 shows B_{final}, the expected field for a coil constructed according to the coefficients in Table I, compared to the modified ideal slowing profile, B_{aug} and a schematic of the tapered coils that produce B_{final}. The difference between

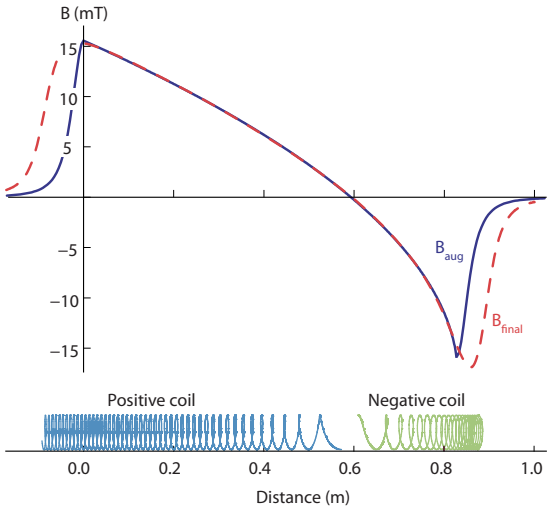

FIG. 3. (Color online) B_{aug}, the ideal magnetic field of Eq. (1) augmented with $1/r^2$ end-correction, and B_{final}, the result of fitting the analytic on-axis magnetic field $B_{helix,z}$ from Eq. (3) to B_{aug} using coefficients shown in Table I. Also shown is a schematic of the tapered coils which generate B_{final}. Note that the effective slowing length was 828 mm, since the field maxima are well inside the physical ends of the tapered coil.

the ideal field B_{ideal} and the analytically calculated field B_{final} is plotted in Fig. 4. The deviation from the ideal slowing profile is very small with some fluctuations evident in the region around the zero crossing where the windings are very sparse and radial components do not cancel perfectly.

The coefficients were determined without considering the small radial components of the field. To evaluate the effects of these radial components and the uniformity of the field over the useful near-axis region, the total magnetic field strength $B_{total}=|\mathbf{B}_{helix}|$ was numerically calculated using Eq. (3), 1 cm off-axis, again with the coefficients in Table I. The agreement remains excellent even off-axis with all radial components included; the deviation is below 0.25 mT through the zero-crossing region. The largest deviation occurs at the end of the slower, where the ideal profile has a very steep gradient that could not be obtained with our minimum coil spacing. The atom deceleration will be slightly lower through this section, but because the gradient is below optimum rather than above, atoms will not be decoupled.

Most importantly, all deviations are smooth, ensuring that the field gradient is always very close to that of the ideal

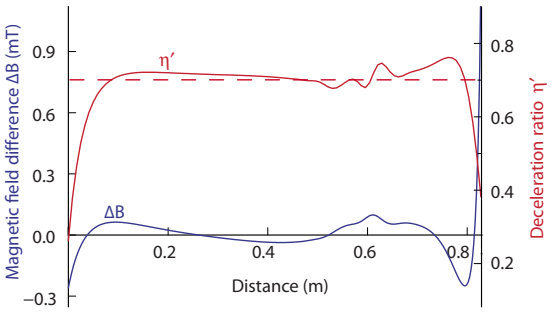

FIG. 4. (Color online) The difference between the ideal field B_{ideal} and analytically calculated field B_{final}, $\Delta B=B_{ideal}-B_{final}$, as a function of position along the Zeeman slower, and the ratio of predicted deceleration to ideal on-resonance deceleration, η'. Design parameter $\eta=0.7$ (dashed line).

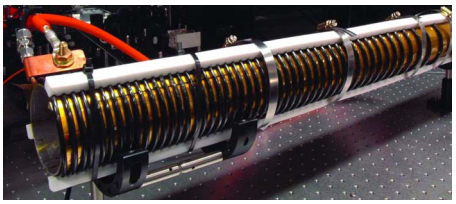

FIG. 5. (Color online) Photograph of the enameled, positive tapered coil wrapped on a stainless steel support tube and clamped in place by three machined PTFE guides. The water cooling and current connections are also visible.

profile. Figure 4 shows η', the calculated ratio of deceleration to the ideal on-resonance deceleration a predicted from B_{final}. η' is very close to the chosen design parameter value $\eta=0.7$ and remains below $\eta'=0.8$ for the entire length of the Zeeman slower. The deviations are small compared with those of most multilayered coils, emphasizing the relatively small curvature of the field from a single coil design.

The Zeeman slower was designed to decelerate atoms from an initial velocity of 365 m/s, thus capturing half of the thermal distribution of atoms from an effusive oven operating at 120 °C. For a final velocity of 20 m/s and a design parameter of $\eta=0.7$, the length of the Zeeman slower was 83 cm.

D. Coil construction

A 1 m long, 77 mm diameter stainless steel tube supported the two helical coil sections of the Zeeman slower. The support tube slides over the outer diameter of a standard DN40CF flange, allowing the end of the Zeeman slower to be positioned as close to the MOT as possible. The relatively large diameter compared with the 40 mm vacuum tube diameter improves the field off-axis homogeneity, at the expense of increased power requirements and dissipation.

The helices were wound onto the support tube using templates calculated from Eq. (2) using the coefficients in Table I. The templates were generated by taking the 2π modulus of the angle $\theta(p)$, effectively unwrapping each helix onto a two-dimensional plane. The templates were printed to scale and wrapped around the stainless steel tube, creating an exact pattern for the coils. Two lengths of hollow copper refrigerator tubing (4 mm outside diameter and 2.8 mm inside diameter) were wrapped around the tube following the templates for the positive and negative coils. The coils were then removed and enameled for electrical insulation. A layer of polyimide film was added between the stainless steel tube and the enameled coils to provide additional electrical insulation. A set of three guides were used to hold the coil in place (see Fig. 5). 4 mm slots with semicircular profiles were machined into bars of PTFE (polytetrafluoroethylene) at the exact angles and positions to hold each turn of the coils in place. Resistive wire for bake-out heating was wrapped onto the vacuum tube and insulated, before sliding on the support tube and Zeeman coil. Bake-out to temperatures of 400 °C has been achieved while running cooling water through the coil to ensure the enamel was not heated above its maximum rating of 150 °C.

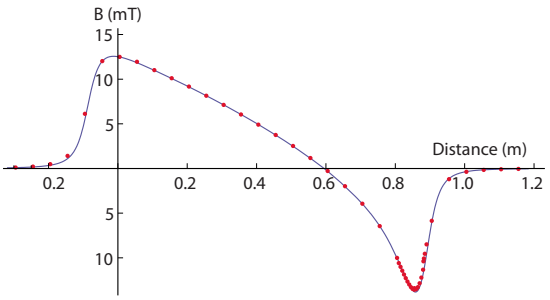

FIG. 6. (Color online) On-axis Hall probe measurements (filled circles) compared to analytically calculated on-axis magnetic field amplitude B_{fit} (solid line) for a current of 90 A. The difference was less than 0.1 mT (1% of the field maximum) over the entire slowing region.

The measured[28] on-axis magnetic field profile shows excellent agreement with the analytically calculated field amplitude B_{final} (Fig. 6). The difference was less than 0.1 mT (1% of the field maximum) over the entire slowing region. Closely spaced (5 mm) measurements near the minimum of the negative coil show the smoothness of the field.

The calculated inductance of the coil, for 68 turns in 96 cm with radius $R=38.3$ mm is 30 μH. The inductance measured with an ac bridge was $L=38$ μH and 20 μH at 1 and 10 kHz, about three orders of magnitude smaller than a multilayer Zeeman slower we have previously used for rubidium (length 50 cm, 25 layers, $L=114$ mH, and 94 mH). The small inductance allowed us to switch the field with a rise time of less than 300 μs, as measured using a Hall probe.

E. Slowing laser and optical probes

Rubidium-85 atoms were slowed by light tuned 260 MHz below the $5S_{1/2}F=3 \rightarrow 5P_{3/2}F=4$ cycling transition, and a repump light field tuned to the equivalent Zeeman-shifted $5S_{1/2}F=2 \rightarrow 5P_{3/2}F=3$ transition, adjusted to optimize the slow atom flux. The slower and repump laser beams were both σ^- polarized relative to their direction of propagation. Two separate external cavity diode laser (ECDL) (Ref. 29) beams were coupled into one single mode fiber and then into a semiconductor tapered amplifier to create a combined field in which the two components were spatially mode-matched. The tapered amplifier produced up to 400 mW of power, though 60 mW was more than sufficient for normal operation with equal power in the slowing and repump laser beams. The slowing laser beam was focused near the exit aperture on the cold cup to reduce transverse spreading.[30]

The atomic beam velocity distribution was measured using the Doppler dependence of a nearly counterpropagating fluorescence probe. The probe ECDL was operated near the $5S_{1/2}F=3 \rightarrow 5P_{3/2}F=4$ transition. The 3 mW probe beam entered the vacuum chamber through the same port as the Zeeman slower beam, crossing the atomic beam 20 cm from the end of the tapered coil to avoid Zeeman shifts in the probe-atom interactions (Fig. 7). The probe crossed at 168° to the atomic beam to obtain a large Doppler dependence and therefore high velocity resolution. The fluorescence was detected using a lens and photomultiplier tube perpendicular to both atomic and probe beams.

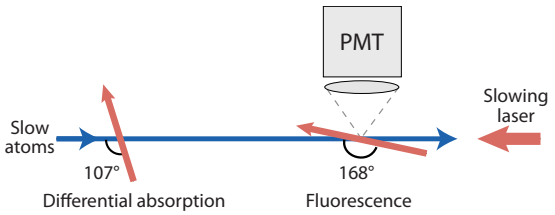

FIG. 7. (Color online) Schematic of the optical probe configuration for characterizing the atomic beam. The fluorescence probe was located far from the end of the slower to avoid Zeeman shifts in the probe region and at a small angle to the atomic beam to provide high velocity resolution. The absorption probe, nearly perpendicular to the atomic beam, provided quantitative measurement of the flux. PMT: photomultiplier tube.

An absorption probe was used for quantitative measurement of the total atomic beam flux. The absorption probe beam (150 μW) was incident at 107° to the atomic beam to increase the absorption signal at the expense of velocity resolution. The absorption signal was obtained using a Hobbs auto-balanced photodetector.[31] The atom density was calculated using the atomic beam diameter, assumed to be equal to the diameter of the slowing laser at the point where the absorption probe intersected the atom beam.

III. RESULTS

Figure 8 shows the frequency dependence of the fluorescence as the probe was scanned. The frequency was calibrated by saturated absorption spectroscopy of a reference vapor cell and converted to a velocity scale using the calculated Doppler shift of the probe. The Zeeman slower was tuned to a final atomic velocity of 35 m/s by adjusting the current in the positive and negative coils to 110 and 90 A, respectively, with a total power dissipation of 700 W. The data show a strong slow-atom signal at 35 m/s with three peaks corresponding to the $F=4$, 3, and 2 hyperfine levels of the excited state. Note the $F=3$ and $F=2$ atoms are not at higher velocities, but frequency shifted due to the excited state hyperfine splitting. The dip in the $F=3$ hyperfine peak is an electromagnetically induced transparency (EIT) resonance[32] due to coherent coupling between the repump and probe lasers. The oven temperature for this measurement was 80 °C at the reservoir and 100 °C at the collimation tube, while using 40 mW of combined optical slowing and repump power.

The atomic flux was measured for the same conditions using the differential absorption probe. The measured flux

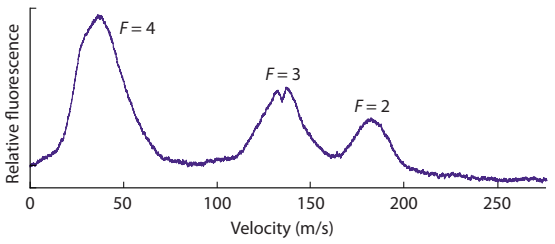

FIG. 8. (Color online) Frequency dependence of the fluorescence probe showing slow atoms at 35 m/s in three peaks corresponding to decay from the $F=4,3,2$ excited state hyperfine levels. The dip in the $F=3$ peak is due to an EIT resonance between the repump and probe laser fields.

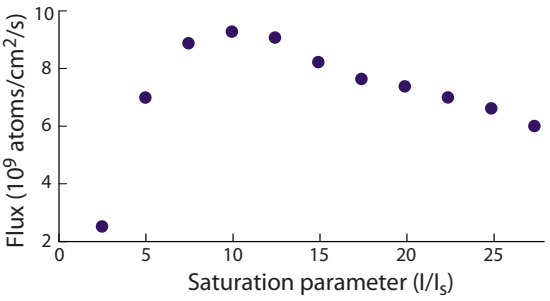

FIG. 9. (Color online) Variation of flux of 35 m/s atoms with slowing laser intensity. The decrease for higher intensities is due to broadening of the slow atom peak, caused by saturation broadening of the transition. The intensity values are for the slowing laser component of the field only, calculated using the radius of the slowing laser beam at the midpoint of the slower (10 mm). The reservoir and collimation tube temperatures for these data were 120 and 145 °C, respectively.

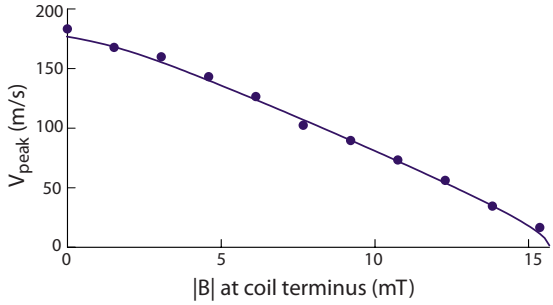

FIG. 10. (Color online) Variation of peak velocity of the slow atoms as the difference in magnetic field between the beginning and end of the Zeeman slower was changed. Only the current in the negative coil was altered so that the initial capture velocity was unchanged; that is, $|B|=0$ means there was no current in the negative coil. The solid line is the result of a simple theoretical model calculating the deceleration based on the resonance condition of the atom-photon interaction.

was 5×10^9 cm^{-2} s^{-1}, and increased approximately linearly with collimation tube temperature up to the maximum measured value of 2×10^{10} cm^{-2} s^{-1} at a temperature of 200 °C, comparable with other Zeeman-slowed effusive Rb sources.[3] The flux was more sensitive to the temperature of the collimating tube than the rubidium reservoir, suggesting that the tube not only collimates the beam but acts as an effective source of atoms.

The laser power also affected the flux, as shown in Fig. 9. The flux of atoms traveling at 35 m/s increased rapidly with power, reaching saturation at $I/I_s=10$, where I is the slowing laser intensity (not including repump) and I_s is the saturation intensity, 1.85 mW/cm^2. As the power was further increased, the peak flux (35 m/s) decreased as saturation of the transition broadened the velocity distribution. Although the peak flux decreased, the integrated flux of slow atoms continued to increase up to the highest measured intensity.

The positive coil current determines the maximum initial velocity of atoms that can be slowed, and thus the flux of atoms reaching the zero-crossing region. Increasing the current will increase the flux, until losses due to atoms decoupling from the laser field outweigh the gains from the increased capture fraction. Although both coils were designed to run at 110 A, we found the atomic flux at 35 m/s still increasing as the positive coil was increased to 125 A, the limit of our power supply.

The current in the negative coil determines the final velocity of the atoms as they leave the slower. This section of the slower was found to be sensitive to the current and slowing laser detuning. The final flux was strongly dependent on the repump laser frequency, which was tuned carefully to ensure atoms remained coupled through the zero crossing. To achieve the maximum fluorescence signal, the repump laser frequency was slightly increased as the current in the negative coil was increased. While the negative section was also designed to run at 110 A, the flux decreased dramatically as the current was increased above 100 A. The sharp reduction in signal is attributed to transverse spreading and reversing of the atoms through the terminating magnetic field.[33]

Figure 10 shows the final peak velocity as the current in the negative coil was increased, and the final velocity was tuned from 183 m/s to 17 m/s. The current in the positive coil was maintained at 110 A with the slowing laser locked 265 MHz below the $F=3\rightarrow F=4$ transition, and the repump laser frequency was adjusted to optimize the slow atom flux. The measured results are compared with a simple theoretical model that integrates the deceleration based on the resonance condition of the atom-photon interaction to find the velocity at the end of the slower.[27] The intensity of the slowing laser field was used as a scaling parameter to adjust the simulation to the data. The agreement is best for a value of $I/I_s=5$, consistent with the slowing laser power (20 mW) and diameter (10 mm $1/e^2$) of the slowing laser beam.

IV. CONCLUSION

The effusive oven with collimation tube, and the variable pitch single-layer Zeeman slower, provide a reliable, low-maintenance and easily constructed source of slow atoms for experiments including MOTs and Bose–Einstein condensates. The single-layer Zeeman coil was simple to construct and adjustable, and also reduced the coil inductance by three orders of magnitude compared with an equivalent multilayer coil. Two similar sources have been constructed, demonstrating high reliability and consistent performance. The emphasis in the design is on utility rather than performance, in particular the ease of construction and maintenance. The final flux of 35 m/s slow atoms was 2×10^{10} cm^{-2} s^{-1} for an oven temperature of 200 °C, comparable to other slow atom sources, and greater flux should be possible if required.

[1] E. L. Raab, M. Prentiss, A. Cable, S. Chu, and D. E. Pritchard, Phys. Rev. Lett. **59**, 2631 (1987).
[2] H. J. Metcalf and P. Van der Straten, *Laser Cooling and Trapping* (Springer, New York, 1999).
[3] E. W. Streed, A. P. Chikkatur, T. L. Gustavson, M. Boyd, Y. Torii, D. Schneble, G. K. Campbell, D. E. Pritchard, and W. Ketterle, Rev. Sci. Instrum. **77**, 023106 (2006).
[4] Z. T. Lu, K. L. Corwin, M. J. Renn, M. H. Anderson, E. A. Cornell, and C. E. Wieman, Phys. Rev. Lett. **77**, 3331 (1996).
[5] S. Chaudhuri, S. Roy, and C. S. Unnikrishnan, Phys. Rev. A **74**, 023406 (2006).
[6] W. DeGraffenreid, J. Ramirez-Serrano, Y.-M. Liu, and J. Weiner, Rev. Sci. Instrum. **71**, 3668 (2000).
[7] P. Cren, C. F. Roos, A. Aclan, J. Dalibard, and D. Guéry-Odelin, Eur. Phys. J. D **20**, 107 (2002).
[8] Y.-J. Lin, R. L. Compton, I. B. Spielman, and J. V. Porto, Phys. Rev. A **79**,

063631 (2009).
[9] M. R. Walkiewicz, P. J. Fox, and R. E. Scholten, Rev. Sci. Instrum. **71**, 3342 (2000).
[10] C. Slowe, L. Vernac, and L. V. Hau, Rev. Sci. Instrum. **76**, 103101 (2005).
[11] A. Pailloux, T. Alpettaz, and E. Lizon, Rev. Sci. Instrum. **78**, 023102 (2007).
[12] H. C. W. Beijerinck and N. F. Verster, J. Appl. Phys. **46**, 2083 (1975).
[13] MDC part no. 400000. The inner diameter through the flanges was increased slightly to allow free insertion of the ampule. Note: commercial equipment, instruments, or materials are identified in this paper in order to adequately specify the experimental procedure. Such identification does not imply recommendation or endorsement, nor does it imply that the materials or equipment are necessarily the best available for the purpose.
[14] Uniblitz shutter part no. VS14S1T0L.
[15] R. E. Scholten, Rev. Sci. Instrum. **78**, 026101 (2007) (hard drive from Apple iPod).
[16] Duniway Stockroom Corp. part no. CA-275.
[17] V. S. Bagnato, G. P. Lafyatis, A. Martin, K. Helmerson, J. Landry, and D. E. Pritchard, J. Opt. Soc. Am. B **6**, 2171 (1989).
[18] R. J. Napolitano, S. C. Zillio, and V. S. Bagnato, Opt. Commun. **80**, 110 (1990).
[19] S. K. Mayer, N. S. Minarik, M. H. Shroyer, and D. H. Mclntyre, Opt. Commun. **210**, 259 (2002).
[20] W. D. Phillips and H. Metcalf, Phys. Rev. Lett. **48**, 596 (1982).
[21] A. Witte, T. Kisters, F. Riehle, and J. Helmcke, J. Opt. Soc. Am. B **9**, 1030 (1992).
[22] F. Lison, P. Schuh, D. Haubrich, and D. Meschede, Phys. Rev. A **61**, 013405 (1999).
[23] T. E. Barrett, S. W. Dapore-Schwartz, M. D. Ray, and G. P. Lafyatis, Phys. Rev. Lett. **67**, 3483 (1991).
[24] K. M. R. van der Stam, E. D. van Ooijen, R. Meppelink, J. M. Vogels, and P. van der Straten, Rev. Sci. Instrum. **78**, 013102 (2007).
[25] K. J. Günter, Ph.D. thesis, Ecole Normale Supérieure, 2004.
[26] D. Steck, Rubidium 85 D line data (Revision 0.2, 1 September 2008).
[27] C. J. Dedman, J. Nes, T. M. Hanna, R. G. Dall, K. G. H. Baldwin, and A. G. Truscott, Rev. Sci. Instrum. **75**, 5136 (2004).
[28] Hirst Magnetic Instruments Ltd. GM08 Gaussmeter.
[29] C. J. Hawthorn, K. P. Weber, and R. E. Scholten, Rev. Sci. Instrum. **72**, 4477 (2001).
[30] M. Prentiss, A. Cable, and N. P. Bigelow, J. Opt. Soc. Am. B **6**, 2155 (1989).
[31] P. C. D. Hobbs, Appl. Opt. **36**, 903 (1997).
[32] S. A. Hopkins, E. Usadi, H. X. Chen, and A. V. Durrant, Opt. Commun. **138**, 185 (1997).
[33] J. V. Prodan, W. D. Phillips, and H. Metcalf, Phys. Rev. Lett. **49**, 1149 (1982).